BILINGUAL PUBLISHING CO.
Pioneer of Global Academics Since 1984

Non-Metallic Material Science
https://ojs.bilpublishing.com/index.php/nmms

ARTICLE

High Energy X-Ray Dosimetry Using $(ZnO)_{0.2}(TeO_2)_{0.8}$ Thin Film-based Real-time X-Ray Sensor

M.M. Idris[1,2,3*], I.O. Olarinoye[1], M.T. Kolo[1], S.O. Ibrahim[1], and J.K. Audu[4]

[1] *Department of Physics, Federal University of Technology, P.M.B 65, Minna, Nigeria*
[2] *Department of Physics, Nasarawa State University, P.M.B 1022, Keffi, Nigeria*
[3] *Department of Physics, University Putra, 43400, Malaysia*
[4] *Department of Medical Physics and Radiotherapy, National Hospital, P.M.B 425, Abuja, Nigeria*

ABSTRACT

This study reports the dosimetric response of a $(ZnO)_{0.2}(TeO_2)_{0.8}$ thin film sensor irradiated with high-energy X-ray radiation at various doses. The spray pyrolysis method was used for the film deposition on soda-lime glass substrate using zinc acetate dehydrate and tellurium dioxide powder as the starting precursors. The structural and morphological properties of the film were determined. The I-V characteristics measurements were performed during irradiation with a 6 MV X-ray beam from a Linac. The results revealed that the XRD pattern of the AS-deposited thin film is non-crystalline (amorphous) in nature. The FESEM image shows the non-uniform shape of nanoparticles agglomerated separately, and the EDX spectrum shows the presence of Te, Zn, and O in the film. The I-V characteristics measurements indicate that the current density increases linearly with X-ray doses (0-250 cGy) for all applied voltages (1-6 V). The sensitivity of the thin film sensor has been found to be in the range of 0.37-0.94 $mA/cm^2/Gy$. The current-voltage measurement test for fading normalised in percentage to day 0 was found in the order of day 0 > day 15 > day 30 > day 1 > day 2. These results are expected to be beneficial for fabricating cheap and practical X-ray sensors.

Keywords: Thin film; X- ray radiation; I-V characteristics; Dosimetry

*CORRESPONDING AUTHOR:
M.M. Idris, Department of Physics, Federal University of Technology, P.M.B 65, Minna, Nigeria; Department of Physics, Nasarawa State University, P.M.B 1022, Keffi, Nigeria; Department of Physics, University Putra, 43400, Malaysia; Email: idrismustapham@nsuk.edu.ng

ARTICLE INFO
Received: 27 December 2022 | Revised : 30 December 2022 | Accepted: 2 February 2023 | Published Online: 16 February 2023
DOI: https://doi.org/10.30564/nmms.v5i1.5369

CITATION
Idris, M.M., Olarinoye, I.O., Kolo, M.T., et al., 2023. High Energy X-Ray Dosimetry Using $(ZnO)_{0.2}(TeO_2)_{0.8}$ Thin Film-based Real-time X-Ray Sensor. Non-Metallic Material Science. 5(1): 4-13. DOI: https://doi.org/10.30564/nmms.v5i1.5369

1. Introduction

The continuous expansion of ionising radiation applications in many areas has necessitated the use of dosimeters with special physical features, such as small size [1]. The quest to design miniaturised dosimeters with small active volumes has consequently led to increasing research into materials in thin film form for their dosimetric properties [2-4]. Numerous techniques of deposition, both physical and chemical, have been adopted for transparent conducting oxide thin film preparation. The desired properties of the prepared film are predetermined by the deposition technique used. These can greatly affect the functionality of the film device [5].

The widespread usage of transparent conducting oxide (TCO) thin films in optoelectronic devices such as touch screens, liquid crystal displays, solar cells, and light-emitting diodes in recent years has drawn substantial scientific interest [6,7]. Owing to its strong electrical conductivity and excellent transparency to visible light, indium tin oxide (ITO) is the most widely used TCO [8]. The high price, limited supply, and toxicity of indium, the main component of ITO, have raised significant concerns about finding viable substitutes [9]. In addition, ITO loses some of its electrical and optical qualities when exposed to a hydrogen plasma environment [10].

Due to its excellent optical and electrical characteristics as well as the low cost, non-toxicity, and abundance of Zn, ZnO is a particularly alluring material in this respect and a great substitute material for ITO [11]. At ambient temperature, ZnO is an n-type semiconductor material with a relatively broad band gap energy of 3.37 eV and a significant exciton-binding energy (60 meV) [12]. High thermal stability, strong stability in hydrogen plasma, and high electrochemical stability are some of its additional advantageous characteristics when compared to ITO [11,13].

Tellurium oxide is a p-type semiconductor material with a band gap of about 2.88 eV and interesting non-linear optical properties [14]. It is characterised by a high dielectric constant in both crystal and film making it a potential candidate for future use in ultra-high integrated electronic devices [15]. TeO_2 based materials have attracted considerable research interest in recent years due to their high refractive index, good non-linear optical properties and electrical semi-conductivity appealing for various applications [16].

Transparent conducting oxide has been reported to be deposited on substrates using a variety of deposition techniques, including pulse laser deposition (PLD) [17], chemical vapour deposition (CVD) [18], radio frequency (RF) sputtering [19], and the sol-gel method [20]. RF sputtering method and convoluted deposition techniques, like MBE, showed good thin film defect density, crystal structure consistency, and high deposition speeds with little defect concentration [19]. The deposition technique, however, costs more than conventional deposition techniques while producing high deposition rates. The spray pyrolysis method can produce high-quality thin films on substrates at moderate temperatures with a low cost of operation [21-31].

With regard to the lattice characteristics and thermal mismatching between the substrate and the film owing to the development of stress in the deposited films, the choice of substrate material is crucial for the formation of ZnO doped TeO_2 thin films [24]. Aside from that, the type of substrate can also affect how ZnO film nucleates and grows. Soda-lime glass [25], sapphire (Al_2O_3) [26], Si (1 0 0) [9], and GaAs [27] are examples of substrates often employed for the deposition of a most metal oxide including ZnO and TeO_2 thin films. Among the substrate materials, soda-lime glass substrate has been proven suitable [29-36]. In this study, we prepared a $(ZnO)_{0.2}(TeO_2)_{0.8}$ thin film sensor by spray pyrolysis with the aim of testing the dosimetric response during irradiation with high-energy x-rays.

Thin film sensor undergoes structural changes when exposed to ionising radiation such as optical, structural and electrical properties [29]. Ionizing radiation can cause changes in the properties of the thin film which depend on the radiation dose, parameters associated with the films, and the radiation type [7,30-32]. Previous studies have investigated materials in thin film form as radiation sensors for conceivable dosimeter designs [29-37]. For gamma sens-

ing and dosimetry application, In_2O_3 thin film was recently deposited using the spray pyrolysis method and optimised [33]. It was discovered that the deposition conditions affected the film's gamma-ray sensitivity. The investigation came to the conclusion that the thin films are suitable for use as photon dosimeters. However, the toxic nature of indium oxide [34] could prevent the widespread manufacture of dosimeters based on the substance. Another study [35] discovered that polymer-encased CS_4PbI_6 thin films were extremely sensitive to X-rays, reaching 256.20 cu cm^{-2} for 30 keV X-rays at a bias voltage of 10 V. The materials were determined to be reliable, strong, and reusable for radiation measurement. The effects of gamma photon irradiation on the crystallinity, microstructure, optical transmission, and photoluminescence characteristics of PbIn thin films deposited by the spin coating process were also reported by Aldawood et al. [35]. The examined film's characteristics were discovered to change with photon exposure and may be calibrated for radiation monitoring and detection. Other thin film materials, including ZTO [37], ZrO_2 [36], MoO_3 [38], ZnO [39], ITO [40], TeO_2 [41], and others, have shown properties that make them highly sensitive to radiation and, as a result, appropriate for the fabrication of real-time dosimeters.

When subjected to photons, ZnO and TeO_2 have each individually demonstrated changes in their optical, structural, and electrical characteristics [16,39,41]. These findings show that both materials are highly photon sensitive due to their electrical and optical characteristics. However, it could be possible to maximise radiation sensitivity by combining both materials in thin film form. As a result, for the first time, this study will look at how the electrical characteristics of $(ZnO)_{0.2}(TeO_2)_{0.8}$ composite thin films are altered for X-ray photon detection and dosimetry. The fabrication of thin-film-based miniaturized dosimeters that is extremely sensitive, stable, repeatable, reusable, and capable of real-time readout in radiation-related applications such as medicine was the motivating factor behind this study. This study aims to investigate and evaluate the effects of various X-ray doses on the current-voltage (I-V) properties of the $(ZnO)_{0.2}(TeO_2)_{0.8}$ thin film sensor, as well as the sensitivity and lowest detectable dosage at various bias voltages.

2. Experimental procedure

2.1 Chemical synthesis

The zinc acetate dehydrate was slowly added (drop-wise) into a beaker placed on an analytical balance until 0.863 g was measured, then 2.0 mL of acetyl acetone and 58.0 mL of methanol were added, respectively. The mixture was stirred vigorously using a magnetic stirrer for about 15 minutes at room temperature until the solute completely dissolved. Also, 0.638 g of tellurium dioxide solute with a molecular weight of 159.6 g/mol was measured and then dissolved in 40 mL of HCl (43 mol% concentration) and 20 mL of methanol, respectively. The solution was vigorously mixed while being heated at 60 °C for about 15 minutes using a magnetic stirrer hotplate, until the solute dissolved completely. The addition of methanol to the tellurium dioxide solution was to prevent precipitation.

2.2 Thin film deposition

Spray pyrolysis was used to create the $(ZnO)_{0.2}(TeO_2)_{0.8}$ thin film sensors. Compressed air was employed as a carrier gas to spray the atomized precursor solution of ZnO-doped TeO_2 onto a heated soda-lime glass substrate using a desktop-style automated ultrasonic spray pyrolysis coating apparatus (U-spray USP 1500). 10 mL of the precursor solution was placed in the dispensing tank of the depositor, and the substrate temperature was maintained at 300 °C throughout the deposition procedure. The flow rates of the solution, air, and the distance from the nozzle to the substrate are 0.15 mL·min^{-1}, 0.2 kg·cm^{-2}, and 3.0 cm, respectively. An innate solution tube and a glass tube, through which carrier gases travel, make up the spray nozzle. The solution is automatically sucked in and then sprayed when pressure is applied to the carrier gas, which creates a vacuum at the nozzle's tip. A thin film of thickness 375 nm was created

using 1.2 mL of the synthesised $(ZnO)_{0.2}$ $(TeO_2)_{0.8}$ solution that had been atomized. On the thin film that had been created, a thick film of interdigitated graphite electrodes with an equal inter-electrode spacing of 0.3 mm was printed, together with two copper foils positioned at the margins of the graphite electrodes 10 mm apart from one another. **Figure 1** depicts the schematics diagram of the $(ZnO)_{0.2}(TeO_2)_{0.8}$ thin film sensor that has been constructed.

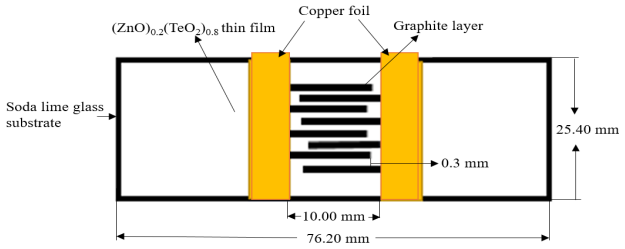

Figure 1. Schematic diagram of the prepared $(ZnO)_{0.2}(TeO_2)_{0.8}$ thin film sensor.

2.3 Characterisation

The film crystallinity and crystalline phase of $(ZnO)_{0.2}(TeO_2)_{0.8}$ thin film was analyzed by X-ray diffraction measurement which was carried out at room temperature by using PHILIPS (PW 3040/60 MPD X'PERT HIGH PRO PANALYTICAL) diffractometer system (scan step of 0.05° (2θ), counting time of 10.16 s per data point) operated at 40 kV and 30 mA. It is equipped with a Cu tube for generating Cu-Kα radiation (k = 1.5406 Å); as an incident beam in the 2-theta mode over the range of 10°-80°. The morphological analysis was performed by FEI (Nova Nanosem 230) field emission scanning electron microscope (FESEM). Energy-dispersive spectrum (EDX) analysis of the film was performed during FESEM measurements.

2.4 Irradiation and I-V characteristic determination

The $(ZnO)_{0.2}(TeO_2)_{0.8}$ thin film sensor was exposed to various doses (dose rate) of 50 cGy (200 cGy), 100 cGy (250 cGy/min), 150 cGy (300 cGy/min), 200 cGy (350 cGy/min), and 250 cGy (400 cGy) X-ray at an exposure time of 0.25, 0.4, 0.5, 0.57, 0.63 min, respectively, using a 6 MV photon beam linear accelerator (Elekta Synergy Platform). The thin film was positioned such that it was parallel to the X-ray beam. Secondary charged particle equilibrium was implemented using an additional PMMA build-up layer in front of the thin film sensor, as prescribed by ISO 4037-3 [42]. The irradiation field size of the beam is 5 × 5 cm^2. After the setup, the researcher exits the Linacs bunker, and in accordance with a radiation safety policy, waits 60 seconds after the exposure before entering the bunker again. CCTV footage of the bunker and a monitor in the control room that shows the electrometer readings are used to capture the induced current. With regard to the applied voltages of 0, 1, 2, 3, 4, 5, and 6 V, each measurement was done independently.

2.5 Test for dosimetric fading

The I-V characteristics of the thin film sensor were tested for fading. These measurements were performed for post-irradiation of the thin films to high-energy X-rays. The I-V characteristics measurement was carried out at an interval of 0, 1, 2, 15, and 30 days after irradiation respectively. At the end of the I-V characteristics measurements, the values of measured current were normalised to values of day 0 using Equation (1):

$$Normalisation = \frac{I_x}{I_{0x}} \times 100\% \quad (1)$$

where I_x is the measured current at a given day for x voltage and I_{0x} is the measured current at day 0 for x voltage. The normalised values are presented in percentages.

3. Results and discussion

The FESEM images of $(ZnO)_{0.2}(TeO_2)_{0.8}$ thin film are shown in **Figure 2a**. The FESESM was used to image and identify the morphology of the film taken at 50,000× magnification. As we know, ZnO and TeO_2 have a hexagonal and tetragonal structure, respectively, and the FESEM image showed a non-uniform distribution of clustered structures. As

shown in **Figure 2a**, the TeO_2-doped ZnO thin layers are stacked together. As a result, the nanoparticles within the film are seen agglomerated separately in the FESEM image of the film. The nanoparticles are non-uniform in shape, and the grains are non-crystalline and non-uniform. Similar non-uniform surface morphology was reported by Dobri et al. [43] for TeO_2 thin films, Shirpay and Bagheri [44] for $MoTeO_2$ binary thin films, Urfa et al. [45] for ZnO nanoparticles, and Park et al. [46] for TeO_2-core/TiO_2-shell nanowires. Although the samples in the current and previous studies have non-identical morphology and the data differed due to differences in sample preparation, method of deposition, the thickness of the film, chemical sample and post-deposition treatment condition [25,47,48].

The chemical composition of the film was carried out with an energy-dispersive X-ray spectrometer (EDX) during FESEM anaysis. **Figure 2b** shows the EDX spectrum of the $(ZnO)_{0.2}(TeO_2)_{0.8}$ thin film nanostructure, revealing the existence of Te, Zn, and O peaks. After the quasi-quantitative determination of the EDX spectrum, the weight percentages of Te, Zn, and O were 8.09, 5.66, and 28.54, respectively, and the atomic percentages of Te (K), Zn (K), and O were 2.04, 2.78, and 57.32, respectively. It is demonstrated that the purity of the fabrication is high without the other residues such as Si, Ca, and Na derived from the soda-lime glass substrate and Pt buffer layer coating for the FESEM analysis. Traces of Fe in a negligible amount were seen, which might have found their way into the film during Pt coating for FESEM examination. The soda-lime glass substrate residues are relatively high in the EDX spectrum, not as constituents of the film but because of the thin nature of the film (a thickness of 375 nm), which enables the electron to interact with the glass substrate. It is also supposed that the ratio of Zn/O and Te/O_2 is less than 1, compared with the perfect chemical stoichiometry of ZnO and TeO_2. These results reveal that there is some oxygen vacancy in the ZnO/TeO_2 thin film. Similar observations have been reported by Silambarasan et al. [49] and Shanmugam et al. [50].

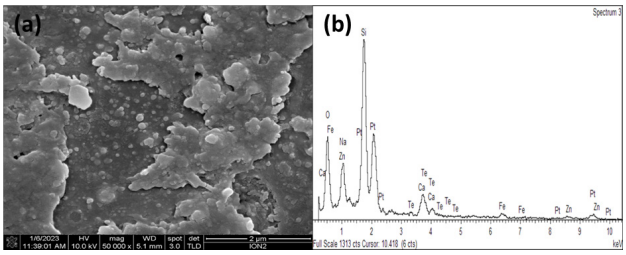

Figure 2. (a) FESEM image of $(ZnO)_{0.2}(TeO_2)_{0.8}$ thin film (b) EDX spectrum of $(ZnO)_{0.2}(TeO_2)_{0.8}$ thin film.

The structural properties of the $(ZnO)_{0.2}(TeO_2)_{0.8}$ thin film were studied by XRD measurement shown in **Figure 3**. The as-deposited thin film is non-crystalline (amorphous) in nature. The pattern shows a highly concentrated weak diffraction peak present at about 23.25° belonging to the diffraction pattern of the α-phase TeO_2 (α-TeO_2, JCPDS card 78-1713) with preferred orientation along (110) direction. A similar XRD diffraction spectrum was reported by Jeong et al. [51] for the dual active layer of IGZO thin film transistor, Khan et al. [52] for as-deposited multilayer ZnO/TiO_2 thin films and Carotenuto et al. [53] for tellurium film. A weak intensive peak at 68.32° is seen which may be due to the wurtzite structure of ZnO (JCPDS card 043-0002) with preferred orientation along (201) direction as reported by Shatnawi et al. [54]. Both α-TeO_2 and wurtzite ZnO phases were already present in the as-deposited $(ZnO)_{0.2}(TeO_2)_{0.8}$ thin film.

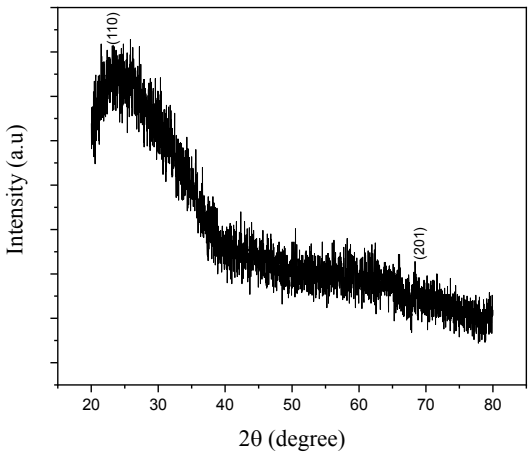

Figure 3. XRD pattern of $(ZnO)_{0.2}(TeO_2)_{0.8}$ thin film.

Figure 4 shows typical current versus applied voltage plots for the $(ZnO)_{0.2}(TeO_2)_{0.8}$ thin film sensor exposed to various X-ray doses. The dependence

of the current density at different voltages applied to the thin film structure is shown in **Figure 5**. Clearly, the current density has been found to increase linearly with the X-ray dose over a range of 0–250 cGy (**Figure 4**). The sensitivities of the $(ZnO)_{0.2}(TeO_2)_{0.8}$ thin film device were calculated using current density versus dose plot and was found to be in the 0.37-0.94 mA/cm^2/Gy range.

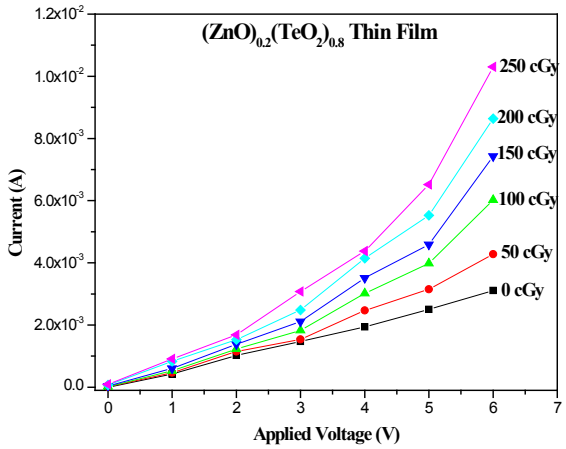

Figure 4. Current versus Voltage (I-V) plot at different X-ray Dose for $(ZnO)_{0.2}(TeO_2)_{0.8}$ thin film device.

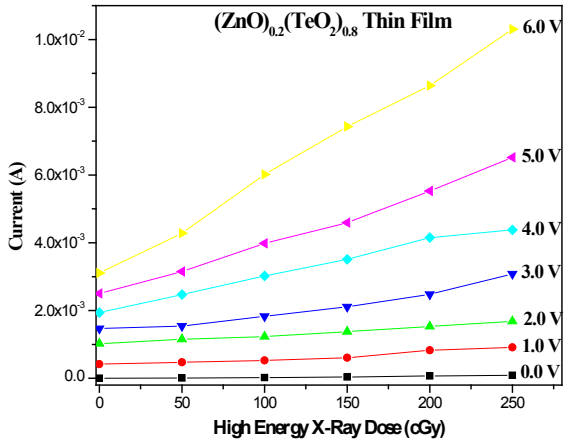

Figure 5. Current versus High Energy X-ray Dose (I-D) plot at different applied Voltages for $(ZnO)_{0.2}(TeO_2)_{0.8}$ thin film device.

The current versus voltage (I-V) characteristics of the prepared thin films show an enhancement in the values of current under a forward-biassed condition. During the transmission of X-rays through thin films, defects are induced, resulting in the disordered structure of the film. This is attributed to the energy transfer from the X-ray radiation dose to the electrons that makes the electron move from the valence band to the conduction band, creating electron-hole pairs that increase the conductivity of the film [16].

The test for fading of the I-V characteristics of the post-X-ray irradiation for days 0, 1, 2, 15, and 30 normalised to day 0 was analyzed. The mean relative readings obtained are in the order of day 0 > day 15 > day 30 > day 1 > day 2. Firstly, there was a decline in the induced current on days 1 (81.59%) and 2 (89.5%). An abrupt increase was observed on day 15 (99.20%) and a slight decrease on day 30 (93.30%). These abnormalities could be attributed to the introduction of ZnO into the lattice of TeO_2 in a small amount (20% ZnO). The semiconducting behaviour of the film indicates that the irradiation with high-energy X-ray radiation affects the microstructure of the film [38-42].

The healing effect may also be responsible for the rise in current density [55]. There are usually some intrinsic flaws created during the film deposition. As a result of the interaction between X-ray radiation and the film, the film's structure will become disorganised throughout transmission through the film. The number of defects (induced plus residual intrinsic defects) is less than the number of intrinsic defects due to the recombination of defects, which lowers the thin film's resistivity and results in an increase in current [56]. At small doses, these thin films have a fine homogeneous grain structure without any large pores. The healing effect may also be used to understand how the critical dosage depends on the film thickness [48]. Therefore, compared to thinner films, larger films require substantially greater radiation doses for healing [29].

Transparent conducting oxide thin layer conductivity control is still a difficult task [38,39]. The optical and electrical characteristics of semiconductor thin film devices can be strongly impacted by even very low concentrations of impurities (down to 10^{-14} cm^3 or 0.01 ppm) and native point defects [57-59]. In order to effectively manage the conductivity in a thin film device, it is essential to comprehend the function of native point defects (such as vacancies, interstitials, and antisites), the integration of impurities, and

the doping of two or more oxides. It has long been confirmed that oxygen vacancies or interstitials are what produce the unintended n-type conductivity in ZnO [60]. Pure ZnO thin films are not resistant to corrosive conditions; for instance, the adsorption of O_2 reduces the film's electrical conductivity and alters the surface shape [61]. In order to make the ZnO system resistant to such changes, doping ZnO with TeO_2 has been examined in this work, leading to the development of an intriguing family of materials based on doped ZnO.

4. Conclusions

This work involves the synthesis, doping, film deposition, structural, morphological study, and the current-voltage characteristics during high energy X-ray exposure of a $(ZnO)_{0.2}(TeO_2)_{0.8}$ thin film sensor prepared by the spray pyrolysis method. The XRD pattern revealed the non-crystalline (amorphous) nature of the film. The FESEM image shows non-uniform shapes of nanoparticles that are agglomerated separately. The current density has been found to increase linearly with the X-ray dose over a range of 0-250 cGy. The sensitivity of the film device was estimated and found to be in the range of 0.37-0.94 $mA/cm^2/Gy$. There is a slight decline in the film conductivity over a period of 30 days after exposure to high-energy X-rays. The semiconducting behaviour of the film indicates that the irradiation with high-energy X-ray doses affects the microstructure of the film. These results are expected to be beneficial for fabricating cheap and practical X-ray detection applications.

Conflict of Interest

There is no conflict of interest.

Acknowledgement

The authors wish to thank the Nigeria government through the Tertiary Education Trust Fund (TET Fund) for funding this research study.

References

[1] Yahaya, I., Mundi, A.A., Mustapha, I.M., et al., 2019. Evaluation of concentration of copper, lead, and zinc in different brands of cigarette sold in Keffi main market of Nasarawa State, Nigeria. Asian Journal of Advance Research and Reports. 4, 1-7. doi: 10.9734/ajarr/2019/v4i430119.

[2] Nie, Y., Xie, Y., Zheng, Y., et al., 2021. Preparation of ZnO/Bi_2O_3 composites as heterogeneous thin film materials with high photoelectric performance on FTO base. Journal of Coatings. 11(9). doi: 10.3390/coatings11091140.

[3] Younus, I.A., Ezzat, A.M., Uonis, M.M., 2021. Preparation of ZnTe thin films using chemical bath deposition technique. Journal of Nanocomposites. 6(4), 165-172. doi: 10.1080/20550324.2020.1865712.

[4] Idris, M.M., Ubaidullah, A., Sulayman, M.B., et al., 2021. Assessment of gamma background exposure levels in some selected residential houses in FCT Abuja , Nigeria. Journal of Radiation and Nuclear Application. 254(3), 251-254.

[5] Edrine, T., Muhammad, D., Ahmad, N.S.Y., et al., 2019. A review: Photonic devices used for dosimetry in medical radiation. Journal of Sensors. 19(1), 2226.

[6] Muchuweni, E., Sathiaraj, T.S., Nyakotyo, H., 2017. Synthesis and characterization of zinc oxide thin films for optoelectronic applications. Journal of Heliyon. 3(4), e00285. doi: 10.1016/j.heliyon.2017.e00285.

[7] Idris, M.M., Olarinoye, I.O., Kolo, M.T., et al., 2022. Transparent conducting oxides thin film dosimetry: Present and the future. Journal of Radiation and Nuclear Application. 7(1), 49-58.

[8] Chen, Y. (editor), 2018. Review of ZnO transparent conducting oxides for solar applications. IOP Conference Series on Material Science and Engineering; 2018 May 25-27; Nanchang, China; UK: IOP Publishing. doi: 10.1088/1757-899X/423/1/012170.

[9] de Godoy, M.P.F., de Herval, L.K.S., Cotta, A.A.C., et al., 2020. ZnO thin films design: The

role of precursor molarity in the spray pyrolysis process. Journal of Material Science: Material in Electronics. 31(20), 17269-17280. doi: 10.1007/s10854-020-04281-y.

[10] Robertson, J., Falabretti, B., 2011. Electronic structure of transparent conducting oxides, 6th ed. Springer US: Boston.

[11] Ilin, E., 2014. Study of the synthesis machanisms and optical properties of ZnO nanomaterials obtained by supercritical fluids route [HAL thesis]. France: Université de Bordeaux.

[12] Eskalen, H., Kavun, Y., Kerli, S., et al., 2020. An investigation of radiation shielding properties of boron doped ZnO thin films. Journal of Optical Materials. 105, 109871. doi: 10.1016/j.optmat.2020.109871.

[13] Khan, Z.R., Khan, M.S., Zulfequar, M., et al., 2011. Optical and structural properties of ZnO thin films fabricated by Sol-Gel method. Journal of Material Sciences and Applications. 2(5), 340-345. doi: 10.4236/msa.2011.25044.

[14] Kariper, A., 2019. Crystalline TeO_2 thin film with chemical bath deposition. Indian Journal of Pure and Applied Physics. 57(3), 175-179.

[15] Bontempo, L., Dos Santos Filho, S.G., Kassab, L.R.P., 2020. Process oxygen flow influence on the structural properties of thin films obtained by co-sputtering of (TeO_2)x-ZnO and Au onto Si substrates. Journal of Nanomaterials. 10(9), 1-16. doi: 10.3390/nano10091863.

[16] Sudha, A., Maity, T.K., Sharma, S.L., et al., 2018. An extensive study on the structural evolution and gamma radiation stability of TeO_2 thin films. Journal of Material Science in Semicondor Processing. 74, 347-351. doi: 10.1016/j.mssp.2017.10.018.

[17] Nistor, M., Rougier, A., 2011. Low temperature Si doped ZnO thin films for transparent conducting oxides. Journal of Solar Energy Materials and Solar Cells. 95, 2357-2362. doi: 10.1016/j.solmat.2011.04.006.

[18] Manzi, J.A., 2016. Zinc precursor synthesis and the aerosol assisted chemical vapour deposition of zinc oxide thin films [PhD thesis]. London: Department of Chemistry University College London Christopher Ingold Laboratories.

[19] Kariper, I.A., 2019. Crystalline TeO_2 thin film with chemical bath deposition. Indian Journal of Pure and Applied Physics. 57(2), 411-419. doi: 10.1007/s00339-021-04344-9.

[20] Bhat, J.S., Maddani, K.I., Karguppikar, A.M., et al., 2007. Electron beam radiation effects on electrical and optical properties of pure and aluminum doped tin oxide films. Journal of Nucear Instruments and Methods in Physics Research B. 258, 369-374. doi: 10.1016/j.nimb.2007.02.074.

[21] Paquin, F., Rivnay, J., Salleo, A., et al., 2015. Multi-phase semicrystalline microstructures drive exciton dissociation in neat plastic semiconductors. Journal of Material Chemistry C. 3, 10715-10722. doi: 10.1039/b000000x.

[22] Arockiam, C.J., Ananthanarayanan, R., Srinivasan, P., et al., 2021. Room temperature selective sensing of benzene vapor molecules using mixed oxide thin film of zinc oxide and cadmium oxide. Journal of Material Science in Semiconduting Processing. 132, 105930. doi: 10.1016/j.mssp.2021.105930.

[23] Saadie, J.H., 2015. Influence of thickness on electrical and optical properties of tellurium thin films deposited by chemical spray pyrolysis. International Journal of Applied Mathematics, Electronics and Computers. 3(2), 96-101.

[24] Xu, S.H., Huang, J.Y., Fei, G.T., et al., 2021. Sol-Gel preparation of high transmittance of infrared antireflective coating for TeO_2 crystals. Journal of Infrared Physics and Technology. 118, 103881. doi: 10.1016/j.infrared.2021.103881.

[25] Patil, N.B., Nimbalkar, A.R., Patil, M.G., 2018. ZnO thin film prepared by a sol-gel spin coating technique for NO_2 detection. Journal of Material Sciences and Engineering B. 227(2), 53-60. doi: 10.1016/j.mseb.2017.10.011.

[26] Özgür, Ü., Ya, I., Alivov, C., et al., 2005. A comprehensive review of ZnO materials and devices. Journal of Applied Physics. 98(4), 1-103. doi: 10.1063/1.1992666.

[27] Look, D.C., 2001. Recent advances in ZnO ma-

terials and devices. Journal of Material Science and Engineering B: Solid-State Materials and Advanced Technology. 80(1-3), 383-387. doi: 10.1016/S0921-5107(00)00604-8.

[28] Kayani, Z.N., Shah, I., Zulfiqar, B., et al., 2017. Structural, optical and magnetic properties of nanocrystalline Co-doped ZnO thin films grown by Sol-Gel. Journal of Applied Physical Sciences. 73(1), 13-21. doi: 10.1515/zna-2017-0302.

[29] Aparna, C., Shetty, P.K., Mahesha, M.G., 2022. Structural optimization of indium oxide thin film for gamma dosimetry applications. Journal of Material Science in Semiconducting Processing. 150, 106931.

[30] Shamma, K., Aldwayyan, A., Albrithen, H., et al., 2021. Exploiting the properties of TiO_2 thin films as a sensing layer on (MEMS)-based sensors for radiation dosimetry applications. Journal of AIP Advanced. 025209, 1-9. doi: 10.1063/5.0032353.

[31] Ogundare, F.O., Olarinoye, I.O., 2015. He + induced changes in the surface structure and optical properties of RF-sputtered amorphous alumina thin films. Journal of Non Crystalline Solids. 432(Part B), 292-299. doi: 10.1016/j.jnoncrysol.2015.10.026.

[32] Olarinoye, I.O., Ogundare, F.O., 2017. Optical and microstructural properties of neutron irradiated RF-sputtered amorphous alumina thin films. Journal of Optics. 134, 66-77.

[33] Jeong, W.S., Kim, J., Seok, J., et al., 2016. Indium oxide (In_2O_3) nanoparticles induce progressive lung injury distinct from lung injuries by copper oxide (CuO) and nickel oxide (NiO) nanoparticles. Journal of Archieves of Toxicology. 90(4), 817-828.

[34] Li, Q., Zhou, C., Nie, S., et al., 2021. Durable Flexible Polymer-Encapsulated Cs_4PbI_6 Thin Film for High Sensitivity X-ray detection. Journal of Nano Letters. 21(24), 10279-10283.

[35] Aldawood, S.M., AlTalib, S., AlGarawi, O.M., et al., 2022. Gamma ray effects on the properties of PbI_2 thin films. Journal of Radiation Physics and Chemistry. 193, 110003.

[36] Chauhan, V.R., Gupta, D., Upadhyay, S., et al., 2022. Influence of high dose gamma radiation on optical, physico-chemical and surface morphology properties of nanocrystalline ZrO_2 thin films. Journal of Optical Materials. 126, 112125.

[37] Wang, S., Uprety, S., Mirkhani, V., et al., 2022. The effect of gamma-ray irradiation on the electrical characteristics of sol-gel derived zinc tin oxide thin film transistors. Journal of Solid-State Electronics. 191, 108270.

[38] Sen, M.A., Manir, S.K., Dutta, M.S., et al., 2020. Influence of total absorbed dose of Co-60 γ-radiation on the properties of h-MoO_3 thin films. Journal of Thin Solid Films. 693, 137700.

[39] Thabit, M.A., Kabir, H.A., Ismail, N.A., et al., 2022. Development of Ag-doped ZnO thin films and thermoluminescence (TLD) characteristics for radiation technology. Journal of Nanomaterials. 12(17), 3068.

[40] Ali, A.M.A., Ahmed, N.M., Mohammad, S.M., et al., 2019. Effect of gamma irradiation dose on the structure and pH sensitivity of ITO thin films in extended gate field effect transistor. Journal of Results in Physics. 12, 615-622.

[41] Maity, T.K., Sharma, S.L., Chourasiya, G., 2012. The real-time gamma radiation dosimetry with TeO_2 thin films. Journal of Radiation Measurements. 47, 145-148. doi: 10.1016/j.radmeas.2011.11.008.

[42] Dubeau, J., Sun, J., Leroux, N., et al., 2023. The HP (3, α) dose response of direct reading survey meters. Journal of Radiation Measurements. 160, 106891. doi: 10.1016/j.radmeas.2022.106891.

[43] Bataliotti, M.D., Costa, F.B., Minussi, F.B., et al., 2022. Characterization of tellurium dioxide thin films obtained through the Pechini method. Journal of Sol-Gel Science and Technology. 1, 378-385. doi: 10.1007/s10971-022-05844-7.

[44] Shirpay, A., Mohagheghi, M.M.B., 2020. Investigation of structural, optical and thermoelectric properties of 2H—$MoTe_2$ and MoO_3—TeO_2 thin films. Journal of Physica B: Condense Matter. 587, 412141. doi: 10.1016/j.physb.2020.412141.

[45] Urfa, Y., Çorumlu, V., Altındal, A., 2021. Gam-

ma ray irradiation dose dependent methanol sensing with ZnO nanoparticles. Journal of Material Chemistry and Physics. 264, 124473. doi: 10.1016/j.matchemphys.2021.124473.

[46] Park, S., An, S., Lee, C., 2013. Structure and photoluminescence properties of TeO_2-core/TiO_2-shell nanowires. Journal of Physica E: Low-dimensional Systems and Nanostructures. 54, 5-8. doi: 10.1016/j.physe.2013.05.023.

[47] Ambedkar, A.K., Singh, M., Kumar, V., et al., 2020. Structural, optical and thermoelectric properties of Al-doped ZnO thin films prepared by spray pyrolysis. Journal of Surfaces and Interfaces. 19, 100504. doi: 10.1016/j.surfin.2020.100504.

[48] Maity, T.K., Sharma, S.L., 2011. Effects of gamma irradiation on electrical, optical and structural properties of tellurium dioxide thin films. Indian Journal of Pure and Applied Physics. 49(9), 606-612.

[49] Silambarasan, M., Saravanan, S., Soga, T., 2015. Raman and photoluminescence studies of A and Fe-doped ZnO nanoparticles. International Journal of ChemTech Research. 7(3), 1644-1650.

[50] Shanmugam, N., Suthakaran, S., Kannadasan, N., et al., 2015. Synthesis and characterization of Te doped ZnO nanosheets for photocatalytic application. Journal of Heterocyclics.1(1), 1-6. doi: 10.33805/2639-6734.105.

[51] Jeong, S., Kim, M., Lee, S., et al., 2014. Dual active layer a-IGZO TFT via homogeneous conductive layer formation by photochemical H-doping. Journal of Nanoscale Research Letters. 9(1), 1-9. doi: 10.1186/1556-276X-9-619.

[52] Khan, M.I., Bhatti, K.A., Qindeel, R., et al., 2016. Investigations of the structural, morphological and electrical properties of multilayer ZnO/TiO_2 thin films, deposited by Sol-Gel technique. Journal of Results in Physics. 6, 156-160. doi: 10.1016/j.rinp.2016.01.015.

[53] Carotenuto, G., Palomba, M., De Nicola, S., et al., 2015. Structural and photoconductivity properties of tellurium / PMMA films. Journal of Nanoscale Research Letters. 10, 313. doi: 10.1186/s11671-015-1007-z.

[54] Shatnawi, M., Alsmadi, A.M., Bsoul, I., et al., 2016. Influence of Mn doping on the magnetic and optical properties of ZnO nanocrystalline particles results in physics influence of Mn doping on the magnetic and optical properties of ZnO nanocrystalline particles. Journal of Results in Physics. 6, 1064-1071. doi: 10.1016/j.rinp.2016.11.041.

[55] Maity, T.K., Sudha, A., Sharma, S.L., et al., 2016. High sensitivity gamma radiation dosimetry using $(In_2O_3)_{0.1}(TeO_2)_{0.9}$ thin films. Journal of Radiation Protection Environment. 1, 135-138. doi: 10.4103/0972-0464.176156.

[56] Sudha, A., Sharma, S.L., Gupta, A.N., 2019. Achieving sensitive and stable indium oxide thin films for gamma radiation monitoring. Journal of Sensors Actuators A: Physica. 285, 378-385. doi: 10.1016/j.sna.2018.10.015.

[57] Chen, C.J., Chandel, A., Thakur, D., et al., 2021. Ag modified bathocuproine: ZnO nanoparticles electron buffer layer based bifacial inverted-type perovskite solar cells. Journal of Organic Electronics. 92, 106110. doi: 10.1016/j.orgel.2021.106110.

[58] Zygmanski, P., 2016. A self-powered thin-film radiation detector using intrinsic high-energy current. Journal of Medical Physics. 43(1), 4-15.

[59] Paraguay D.F., Estrada L.W., Acosta N.D.R., et al., 1999. Growth, structure and optical characterization of high quality ZnO thin films obtained by spray pyrolysis. Journal of Thin Solid Films. 350(1), 192-202. doi: 10.1016/S0040-6090(99)00050-4.

[60] Salam, S., Islam, M., Akram, A., 2012. Sol-gel synthesis of intrinsic and aluminum-doped zinc oxide thin films as transparent conducting oxides for thin film solar cells. Journal of Thin Solid Films. 529, 242-247. doi: 10.1016/j.tsf.2012.10.079.

[61] Al-maiyaly, B.K.H., 2018. Effect of gamma ray irradiation on structural and optical properties of ZnO thin films. Journal of Pure and Applied Science. 28(3).